# The Kinetic Behavior of Chicken Liver Sulfite Oxidase†

Michael S. Brody and Russ Hille*

*Department of Medical Biochemistry, The Ohio State University, 1645 Neil Avenue, 333 Hamilton Hall, Columbus, Ohio 43210-1218*

*Received February 3, 1999; Revised Manuscript Received March 15, 1999*

ABSTRACT: A comprehensive kinetic study of sulfite oxidase has been undertaken over the pH range 6.0−10.0, including conventional steady-state work as well as rapid kinetic studies of both the reaction of oxidized enzyme with sulfite and reduced enzyme with cytochrome *c* (III). A comparison of the pH dependence of $k_{cat}$, $k_{red}$, and $k_{ox}$ indicates that $k_{red}$ is principally rate limiting above pH 7, but that below this pH the pH dependence of $k_{cat}$ is influenced by that of $k_{ox}$. The pH independence of $k_{red}$ is consistent with our previous proposal concerning the reaction mechanism, in which attack of the substrate lone pair of electrons on a $Mo(VI)O_2$ unit initiates the catalytic sequence. The pH dependence of $k_{red}/K_d^{sulfite}$ indicates that a group on the enzyme having a p$K_a$ of ∼9.3 must be deprotonated for effective reaction of oxidized enzyme with sulfite, possibly Tyr 322, which from the crystal structure of the enzyme constitutes part of the substrate binding site. There is no evidence for the $HSO_3^-/SO_3^{2-}$ p$K_a$ of ∼7 in the pH profile for $k_{red}/K_d^{sulfite}$, suggesting that enzyme is able to oxidize the two equally well. By contrast, $k_{cat}/K_m^{sulfite}$ and $k_{red}/K_d^{sulfite}$ exhibit distinct pH dependence (the former is bell-shaped, the latter sigmoidal), again consistent with the oxidative half-reaction contributing to the kinetic barrier to catalysis at low pH. The pH dependence of $k_{cat}/K_m^{(cyt\ c)}$ (reflecting the second-order rate of reaction of free enzyme with free cytochrome) is bell-shaped and closely resembles that of $k_{ox}/K_d^{(cyt\ c)}$, reflecting the importance of the oxidative half-reaction in the low substrate concentration regime. The pH profile for $k_{ox}/K_d^{(cyt\ c)}$ indicates that two groups with a p$K_a$ of ∼8 are involved in the reaction of free reduced enzyme with cytochrome *c*, one of which must be deprotonated and the other protonated. These results are consistent with the known electrostatic nature of the interaction of cytochrome *c* with its physiological partners.

Sulfite oxidase is a complex metalloprotein possessing a molybdenum center and a cytochrome $b_5$ type heme (*1*), responsible for the terminal step in the catabolism of sulfur derived from cysteine, methionine, and membrane components such as the sulfatides. It is localized in the intermembrane space of mitochondria, where reducing equivalents derived from sulfite are passed on to cytochrome *c*, thereby conserving some of the thermodynamic driving force for the reaction in a physiologically useful form. The enzyme belongs to the subclass of mononuclear molybdenum enzymes possessing $LMoO_2$ centers (L being a complex pterin cofactor coordinated to the metal via an enedithiol unit; *1*), which also includes the assimilatory nitrate reductases from higher plants. The overall stoichiometry of the reaction catalyzed is

$$SO_3^{2-} + 2\text{cyt } c^{III} + H_2O \rightarrow SO_4^{2-} + 2H^+ + 2\text{cyt } c^{II}$$

The reductive half-reaction of the catalytic cycle,[1] in which sulfite is oxidized to sulfate and the enzyme is reduced by 2 equiv, occurs at the molybdenum center; the oxidative half-reaction, in which the reducing equivalents thus obtained are subsequently passed on to cytochrome *c*, takes place at the heme. Intramolecular electron transfer from the molybdenum center to the heme is thus an integral aspect of catalysis, as is frequently found to be the case with molybdenum-containing enzymes.

Previous kinetic studies of sulfite oxidase (*2*−*4*) have each provided an incomplete set of steady-state kinetic values for the reaction of beef liver enzyme with sulfite, using either molecular oxygen or cytochrome *c* as electron acceptor. Likewise, an incomplete set of values for the reaction of chicken liver enzyme with sulfite and cytochrome *c* has been provided (*5*). Of these published studies, only Speck et al. (*4*) report data from which a turnover number, $k_{cat}$, of 50 $s^{-1}$ for (bovine) sulfite oxidase can be inferred. In addition, each of these earlier studies has been complicated by the known inhibition of enzyme by high concentrations of anions such as chloride and sulfate (*6*, *7*), underscoring the necessity of controlling anion concentrations in any kinetic study of this enzyme.

The present work describes a series of steady-state and rapid kinetic experiments which have been undertaken in

† This work was funded by a grant from the National Institutes of Health (GM 52322 to R.H.).

* To whom correspondence should be addressed. Phone: 614-292-4964. Fax: 614-292-4118. E-mail: hille.1@osu.edu.

[1] Adopting the standard convention in the enzymological literature concerning oxidoreductase enzymes that possess reversibly reducible prosthetic groups, we refer here to that portion of the catalytic sequence involving the reaction of sulfite with oxidized enzyme to yield the reduced enzyme (and sulfate) as the reductive half-reaction, and that involving the reaction of the reduced enzyme thus obtained with cytochrome *c* to yield oxidized enzyme (and reduced cytochrome *c*) as the oxidative half-reaction.

10.1021/bi9902539 CCC: $18.00 
Published on Web 04/30/1999

an effort to extend our understanding of the reaction of sulfite oxidase. Experiments have been performed over a broad pH range in an effort to determine the effect of pH on the steady-state kinetic behavior of the enzyme, as well as the effect on the individual half-reactions of the catalytic cycle. Our results lend support to a mechanism in which catalysis is initiated by attack of a substrate lone pair on a Mo═O group of the metal center and suggest that Tyr 322 is involved in binding of substrate in the enzyme active site.

## EXPERIMENTAL PROCEDURES

Sulfite oxidase was purified as follows. Fresh chicken liver was obtained from Gerber Poultry Inc., Kidron, OH, or Park Farms, Inc., Canton, OH, and frozen in liquid nitrogen within half an hour of slaughter. The frozen liver was subsequently broken into small pieces and blended to a powder in liquid nitrogen using a metal Waring blender, after which the material was placed in a −20 °C freezer and the liquid nitrogen allowed to evaporate. This powder was either stored at −80 °C or used immediately. To the powder was added 1200−1400 mL of 50 mM potassium phosphate buffer at pH 7.8; this buffer also contained 0.1 mM EDTA,[2] 0.1 mM salicylate, 2 mM sodium molybdate, 0.1 mM PMSF, and 0.3 $\mu$M pepstatin A. The mixture was allowed to thaw to 4 °C, was thoroughly mixed, and then was centrifuged at 700*g* for 1 h. The pellet from this spin was washed with approximately 200 mL of the same buffer as above and recentrifuged at 11300*g* for 30 min. After decanting the supernatant, the pellet was centrifuged again at 17700*g* for 30 min and the supernatants were pooled, discarding the precipitate. The combined supernatant was then centrifuged at 28200*g* for 1 h, strained through glass wool and recentrifuged at 160000*g* for 1 h. The supernatant from this spin is designated as the crude extract. A positive assay for malate dehydrogenase (a marker enzyme for the mitochondrial matrix) demonstrated that the homogenization disrupted even subcellular organelles. To this extract 10% (v/v) butanol (prechilled to −20 °C) was added extremely slowly with constant stirring at 4 °C, followed by powdered ammonium sulfate (11.4 g/100 mL). When the ammonium sulfate was completely dissolved, the mixture was centrifuged at 17700*g* for 30 min and the precipitate was discarded. To the supernatant was added more powdered ammonium sulfate (12.3 g/100 mL), and the mixture was centrifuged again at 17700*g* for 30 min. At this stage, the precipitate contained the crude sulfite oxidase and was retained. The supernatant which still contained xanthine dehydrogenase, could then be precipitated and subjected to further purification as previously published (*8*). The precipitate containing sulfite oxidase was then dissolved in 50 mM potassium phosphate pH 7.8, containing 0.1 mM EDTA, 0.1 mM salicylate, 2 mM molybdate, and 0.1 mM PMSF and dialyzed against 4 L of the same buffer with three changes, over a period of 24 h. The dialyzed solution was centrifuged at 17700*g* for 30 min to precipitate any undissolved protein and then submitted to further purification. The dialyzed solution from the original $(NH_4)_2SO_4$/butanol fractionation (about 350 mL) was applied to a DEAE-sepharose column (3 cm × 32 cm), and the column washed with 1 bed volume of 50 mM Tris, pH 8.0, containing 0.1 mM EDTA and 2 mM molybdate. The column was next washed with 2−3 bed volumes of 50 mM Tris, pH 8.0, containing 0.1 mM EDTA, 2 mM molybdate, and 0.075 M KCl. Finally, the enzyme was eluted with a gradient of 50 mM Tris, pH 8.0, containing 0.1 mM EDTA, 2 mM molybdate, and 0.075 M KCl (350 mL) to 50 mM Tris, pH 8.0, containing 0.1 mM EDTA, 2 mM molybdate, and 0.22 M KCl (350 mL). Fractions of about 9 mL were collected, with sulfite oxidase eluting at about 400 mL. The active fractions were pooled and concentrated to about 10 mL and then applied to a Sephacryl S-200 column (3 cm × 110 cm) equilibrated in 50 mM Tris, pH 8.0, containing 0.1 mM EDTA, 2 mM molybdate, and 0.3 M KCl. Fractions of 6 mL were collected, and the best fractions, based on $A_{414}/A_{280}$ and activity, were pooled and concentrated. The enzyme was next applied to a phenyl-Sepharose column (1.2 cm × 9 cm) which was equilibrated in 50 mM Tris, pH 8.0, containing 0.1 mM EDTA, 2 mM molybdate, and 0.3 M KCl. The column was washed with 1 bed volume of the same buffer and the enzyme eluted with 5 mM Tris, pH 8.0, 0.1 mM EDTA, and 2 mM molybdate. The fractions with an $A_{414}/A_{280}$ of greater than 0.5 were pooled and concentrated. The protein solution was then exchanged by G-25 chromatography into 10 mM potassium phosphate, pH 8.0, containing 2 mM molybdate and applied to a ceramic hydroxylapatite column (1.2 cm × 5 cm) which was eluted with the same buffer. Sulfite oxidase was washed through the column and was collected, whereas contaminating proteins were retained on the column. In a typical preparation, 5.5 mg of enzyme was obtained from 908 g of chicken liver, reflecting an overall yield of enzyme activity present in the crude extract of 23%.

Cytochrome *c* [horse heart (96% pure)], Tris, Bis-Tris, Bis-Tris propane, and glycine were from Sigma. Titanium chloride·HCl (1.8 M) was from Aldrich. Titanium citrate, pH 11, was prepared as described previously (*9*). Ammonium sulfate (Ultrapure) was obtained from ICN Biomedicals and was ground to a fine powder in a blender prior to use. Ceramic hydroxylapatite (type I, 40 $\mu$m) was obtained from Biorad. Sephacryl S-200, Sephadex G-25, DEAE-sepharose, phenyl-sepharose, cytochrome *c* [horse heart (96% pure)] were obtained from Sigma. Ferricenium hexafluorophosphate was prepared as described by Lehman et al. (*10*, *11*). All other chemicals were of reagent grade and used without additional purification.

Sulfite oxidase was routinely assayed at 25 °C in 20 mM Tris buffer, adjusted to pH 8.0 with acetic acid, containing 2 mM sodium molybdate and 0.1 mM EDTA. The aliquots from the crude extract and ammonium sulfate cut were oxidized by exposure to ferricenium hexafluorophosphate prior to being assayed. The reaction was monitored in a Hewlett-Packard 8452A single beam diode array spectrophotometer following reduction of cytochrome *c* at 550 nm—an extinction change of 19 630 $M^{-1}$ $cm^{-1}$ (*12*) was used for the reduction of the cytochrome *c*. This empirically determined number was used because of the lower spectral resolution of the diode array spectrophotometer used in the present work. Protein content was determined by the method of Bradford (*13*).

[2] Abbreviations: Bis-Tris, bis(2-hydroxyethyl)imino-tris[hydroxymethyl)methane; Bis-Tris propane, 1,3-bis[tris(hydroxymethyl)methylaminopropane; DEAE, diethylaminoethyl; EDTA, ethylenediaminetetraacetate; PMSF, phenylmethanesulfonyl fluoride; Tris, tris(hydroxymethyl)aminomethane.

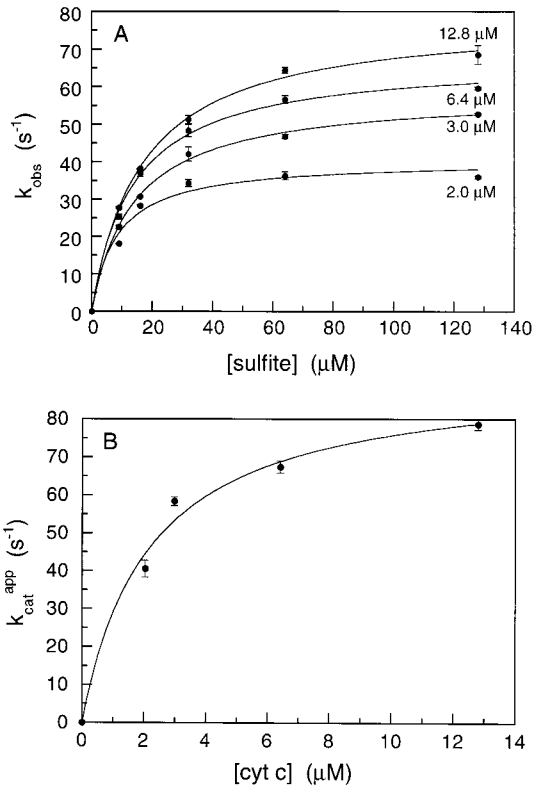


FIGURE 1: Steady-state dependence of catalysis on sulfite. (Panel A) Hyperbolic plots of enzyme rate versus varying concentrations of sulfite (9, 16, 32, 64, and 128 $\mu$M). A separate hyperbolic plot is graphed for each of four different cytochrome *c* concentrations (2.0, 3.0, 6.4, and 12.8 $\mu$M). (Panel B) Plots of the apparent $k_{cat}$ from panel A versus the cytochrome *c* concentration at which it is obtained. The kinetic constants of $k_{cat}$ and the $K_M^{(cytochrome\ c)}$ are obtained by computer fit (as described in the Materials and Methods) from the asymptote of this hyperbola at high [cyt *c*] and the [cyt *c*] yielding half-maximal $k_{cat}$, respectively. Reaction conditions were 0.02 M Tris-acetate buffer, pH 8.0, 25 °C.

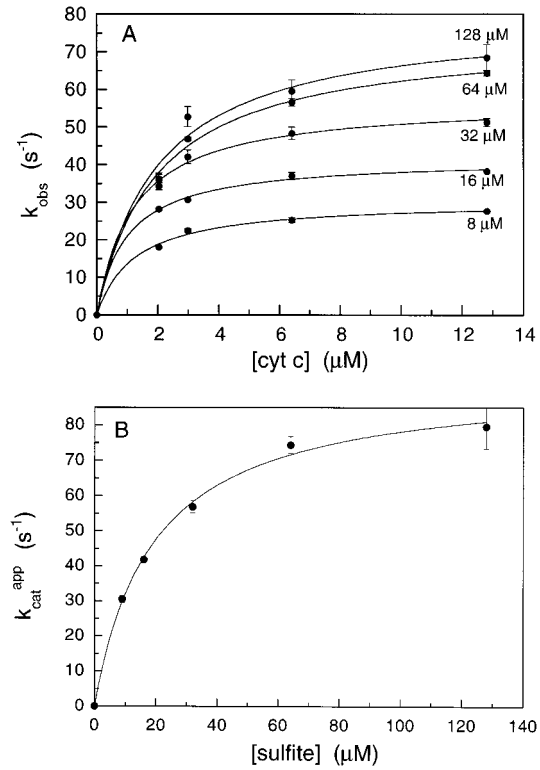


FIGURE 2: Steady-state dependence of catalysis on cytochrome *c*. (Panel A) Hyperbolic plots of enzyme rate versus varying concentrations of cytochrome *c* (2.0, 3.0, 6.4, and 12.8 $\mu$M). A separate hyperbolic plot is graphed for each of five different sulfite concentrations (9, 16, 32, 64, and 128 $\mu$M). (Panel B) A plot of the apparent $k_{cat}$ from panel A versus sulfite concentration. The kinetic constants of $k_{cat}$ and the $K_M^{sulfite}$ are obtained by computer fit (as described in the Materials and Methods) from the asymptote of this hyperbola at high [sulfite] and the [sulfite] yielding half-maximal $k_{cat}$, respectively. Reaction conditions were 0.02 M Tris-acetate buffer, pH 8.0, 25 °C.

Steady-state kinetic measurements were performed aerobically at 25 °C using a 1.0 cm light path cuvette and a final sample volume of 1.0 mL. All experiments were performed with a 20 mM buffer adjusted to the correct pH with acetic acid. The buffers used were Bis-Tris (pH 6.0−6.5), Bis-Tris propane (pH 6.75−7.5), Tris (pH 7.5−8.75), and glycine (pH 8.75−10). To minimize the difficulties with known anion inhibition, all experiments were performed at the same buffer concentration with acetic acid (having an empirically determined $K_I$ toward sulfite oxidase of 254 mM; data not shown) instead of hydrogen chloride ($K_I$ = 4 mM; ref *14*) as the titrant; in each case, less than 35 mM acetic acid was used (i.e., substantially below $K_i$). A full steady-state kinetic study was conducted at pH 8.0 with fresh enzyme and varying concentrations of cytochrome *c* between 1 and 13 $\mu$M and varying concentrations of sodium sulfite between 8 and 130 $\mu$M. The steady-state kinetic pH profile study was conducted using a saturating concentration of cytochrome *c*, 15 $\mu$M (8-fold greater than $K_m$), and varying the concentration of sulfite between 4 and 500 $\mu$M. In constructing this profile, experiments at pH 7.5 and 8.75 were performed in two different buffer systems (Bis-Tris propane and Tris at pH 7.5, and Tris and glycine at pH 8.75) to test whether any buffer-dependent effects might be observed. In both cases, the data were indistinguishable and have simply been averaged in Figures 1 and 2. We note that there are no breaks in any of the pH-dependence plots presented here, and there is no evidence that changing buffers over the extended pH range we have used causes artifacts due to changes in ionic strength.

Rapid reaction studies were performed using either a modified Kinetic Instruments Inc. stopped-flow apparatus equipped with an OLIS Inc. data collection system (reductive half-reaction experiments) or an Applied Photophysics Inc. stopped-flow apparatus (oxidative half-reaction experiments). Kinetic transients observed after mixing enzyme with substrate were monitored as transmittance voltages collected by a high-speed A/D converter and converted to absorbance changes by OLIS or Applied Photophysics software. In the present analyses, it is assumed that intramolecular electron transfer from the molybdenum center to the heme of sulfite oxidase is rapid, as has been shown by Sullivan et al. (*15*); changes in oxidation state of the heme center are thus rate limited by the chemistry taking place at either the molybdenum center (reductive half-reaction) or heme (oxidative half-reaction). Time courses obtained from the stopped-flow were fitted to sums of exponentials using an iterative nonlinear least-squares Levenberg−Marquardt algorithm (*16*). The data were fitted to the expression $\Delta A(t) = \Sigma \Delta A_n \exp(-k_n t)$ for the parameters $\Delta A_n$ and $k_n$ which represent the total absorbance changes and observed rate constants, respectively.

All rapid kinetic experiments were performed anaerobically, with solutions of sulfite oxidase prepared as follows. A total of 25−50 $\mu$L of a concentrated solution of oxidized enzyme was diluted to 6−7 mL with an appropriate buffer of the desired pH. Reductive half-reaction experiments were performed with enzyme which had a final subunit concentration of 0.4−0.8 $\mu$M, while oxidative half-reaction experiments were performed with enzyme which had a final subunit concentration of 1.8−2.2 $\mu$M. The higher concentrations in the oxidative half-reaction were required because (1) the path length for the Kinetic Instruments Inc. apparatus was 2 cm while that for the Applied Photophysics Inc. apparatus was 1 cm, and (2) the larger extinction change of the Soret peak was followed for the reductive half-reaction experiments, while the smaller extinction change of the α peak was followed for the oxidative half-reaction experiments (due to the large interfering absorbance of the Soret peak for cytochrome *c*). After dilution to the desired concentration, the enzyme was then placed in a tonometer equipped with a sidearm cuvette and a three way stopcock, then made anaerobic by repeated evacuation and flushing with $O_2$-free argon. This anaerobic oxidized enzyme was used for the reductive half-reaction experiments. Reduced enzyme for the oxidative half-reaction experiments was prepared by titration of anaerobic, oxidized enzyme with titanium citrate, using the sidearm cuvette attached to the tonometer to follow the reduction spectrophotometrically. Anaerobic solutions of sulfite were prepared by dilution of a concentrated stock solution of sulfite into 10 mL of the appropriate buffer in a 20 mL glass syringe, followed by bubbling for 30 min with $O_2$-free argon. This sample represented twice the highest concentration of sulfite needed for the experiment on the given day. Additional samples of lower concentration were generated by serial dilution of the sulfite stock with anaerobic buffer. In all cases, the lowest concentration remained in pseudo-first-order excess to the enzyme during the experiment. Anaerobic solutions of cytochrome *c* were prepared as follows. Buffer solutions of the appropriate pH were bubbled for 30 min with $O_2$-free argon in 10 mL glass syringes and sealed with rubber septa. After bubbling, varying volumes of 2.3 mM cytochrome *c* in a serum-stoppered vial under an atmosphere of argon were added to 5 mL of anaerobic buffer in the glass syringes to give concentrations between 16 and 140 $\mu$M. The lowest concentration was always at least in 4-fold excess to the enzyme during the experiment. Cytochrome *c* concentrations were confirmed spectrophotometrically. All cytochrome *c* solutions were prepared fresh the day to be used so as to avoid kinetic artifacts associated with aggregation of protein when stored in solution over extended periods of time.

In the case of the oxidative half-reaction, kinetic transients were found to be quite complex, owing to the necessarily sequential nature of the reaction of fully (i.e., three electron) reduced enzyme with three successive equivalents of cytochrome *c*. Rate constants for the fastest phase of the reaction observed at 547 nm and the single phase observed at 562 nm were each integrated over three different time domains for each transient to arrive at a single value which best represents the average rate for the oxidation of enzyme from 3 electron reduced to 2 electron reduced at a given substrate concentration. Intramolecular redox equilibria within partially reduced enzyme between the molybdenum and heme centers may be unfavorable, in that reduction of molybdenum over the heme may be preferred, particularly at low pH, thus decreasing the effective rate of oxidation of two- and one-electron reduced enzyme and complicating analysis of the slower portions of the kinetic transients. This type of kinetic behavior has been observed in other complex redox-active enzymes (*17*, *18*). For these reasons, single-exponential fits over the first ∼70 ms (except pH 6.0 and 10.0, where the first 150−300 ms were used) of the reaction of enzyme with varying concentrations of cytochrome *c* were used in the present work, representing approximately one-third of the total spectral change seen for the reaction and reflecting the reaction of fully reduced enzyme with cytochrome *c*—this value represents the intrinsic rate constant for the electron-transfer reaction.

Hyperbolic substrate concentration dependence was fitted with eq 1 to obtain the corresponding limiting rate parameter ($k_{cat}$, $k_{red}$, or $k_{ox}$) and $K_m$/dissociation constant ($K_d$) (*19*).

$$k_{obs} = k_{lim}[S]/(K_d + [S]) \quad (1)$$

pH profiles for single and double ionizations were fitted to eqs 2 or 3, respectively, to obtain the relevant p$K_a$ values.

$$k_{lim} = [(A^{EH}(10^{(-pH)})) + (A^{E}(10^{(-pKa)}))]/[(10^{(-pH)}) + (10^{(-pKa)})] \quad (2)$$

$$k_{lim}/K_d = T_{max}/[1 + 10^{(pK_{a1}-pH)} + 10^{(pH-pK_{a2})}] \quad (3)$$

Here, $A^{EH}$ and $A^{E}$ represent the intrinsic catalytic activity of the protonated and unprotonated form of the ionization group, respectively; $T_{max}$ represents the theoretical maximal value of the kinetic parameter being fit (in the present example $k_{lim}/K_d$). In the derivation of eq 3, it is assumed that only the middle ionization state (EH in the double equilibrium E = EH = $EH_2$) is catalytically active.

## RESULTS

*Steady-State Kinetics of Sulfite Oxidase.* At pH 8.0, the steady-state oxidation of sulfite to sulfate as catalyzed by sulfite oxidase using cytochrome *c* as the electron acceptor gives plots of initial velocity versus substrate concentration which display typical saturation kinetics with respect to both sulfite and cytochrome *c* (Figure 1). The secondary plots for these data (Figures 1B and 2B, respectively) yield a $k_{cat}$ of 92.6 ± 4.4 $s^{-1}$ (per cytochrome *c*) and $K_m$s of 19.1 ± 1.6 and 2.2 ± 0.5 $\mu$M for sulfite and cytochrome *c*, respectively, at pH 8.0. These $K_m$ values are in good agreement with those previously reported (*2*, *4*−*6*, *20*, *21*), By contrast, $k_{cat}$ is at least twice as large as the literature value (*4*), a difference in all likelihood attributable to our success in minimizing anion inhibition under the present experimental conditions (in which acetic acid at nominal concentrations is used to adjust pH, thus avoiding the more strongly inhibiting chloride of HCl). In analyzing these data, there is a potential concern that the enzyme is inhibited at the higher ionic strengths encountered as the substrate concentration is increased. We note first of all that the inhibition of sulfite oxidase by anions such as chloride and phosphate is due to a specific interaction of these anions with the molybdenum center of the enzyme, mimicking substrate binding, rather than to a generalized

Table 1: Summary of Steady-State Kinetic Parameters across pH Range 6.0−10.0

| pH | $K_M^{sulfite}$ ($\mu$M) | $K_M^{(cytochrome\ c)}$ ($\mu$M) | $k_{cat}$ ($s^{-1}$) | $k_{cat}/K_M^{sulfite}$ ($M^{-1}\ s^{-1}$) | $k_{cat}/K_M^{(cytochrome\ c)}$ ($M^{-1}\ s^{-1}$) |
|---|---|---|---|---|---|
| 6.00 | 10.2 ± 0.98 | 2.2 ± 0.2 | 16.6 ± 0.38 | $1.63 \times 10^6$ | $7.5 \times 10^6$ |
| 6.50 | 10.9 ± 1.0 | ND | 39.2 ± 1.0 | $3.60 \times 10^6$ | ND |
| 6.75 | 12.1 ± 0.55 | ND | 50.4 ± 0.65 | $4.16 \times 10^6$ | ND |
| 7.00 | 11.3 ± 1.6 | ND | 58.6 ± 2.3 | $5.20 \times 10^6$ | ND |
| 7.25 | 10.6 ± 1.7 | ND | 61.8 ± 2.6 | $5.84 \times 10^6$ | ND |
| 7.50 | 11.6 ± 0.97 | ND | 75.3 ± 1.8 | $6.47 \times 10^6$ | ND |
| 7.75 | 11.3 ± 1.2 | ND | 80.0 ± 7.6 | $7.00 \times 10^6$ | ND |
| 8.00 | 16.4 ± 3.0 | 2.2 ± 0.5 | 95.0 ± 1.9 | $5.78 \times 10^6$ | $4.3 \times 10^7$ |
| 8.25 | 17.1 ± 2.3 | ND | 85.5 ± 8.1 | $5.11 \times 10^6$ | ND |
| 8.50 | 31.4 ± 13.0 | ND | 92.0 ± 21.8 | $3.17 \times 10^6$ | ND |
| 8.70 | 50.7 ± 2.3 | ND | 114.3 ± 1.7 | $2.25 \times 10^6$ | ND |
| 8.85 | 57.5 ± 2.2 | ND | 115.3 ± 1.4 | $2.00 \times 10^6$ | ND |
| 9.25 | 97.6 ± 6.1 | ND | 119.4 ± 3.2 | $1.22 \times 10^6$ | ND |
| 9.50 | 108.6 ± 21.3 | 5.5 ± 0.9 | 96.0 ± 11.0 | $9.20 \times 10^5$ | $1.7 \times 10^7$ |
| 10.00 | 118.9 ± 25.2 | ND | 52.6 ± 5.0 | $4.72 \times 10^5$ | ND |

ionic strength effect (*22*−*24*). Second, and more importantly, were such inhibition of sulfite oxidase seen in the present experiments, it would necessarily be manifested in the steady-state plots shown in Figures 1A and 2B as a downward trend at high [sulfite]. As is evident in both these figures, the observed substrate concentration dependence is nicely hyperbolic, and our data demonstrate unequivocally that no inhibition is observed over the sulfite concentration range used in the present study.

To gain insight into the effect of pH on the reaction of sulfite oxidase, two sets of experiments were performed. In the first, the concentration of cytochrome *c* was varied while that of sulfite was held constant at 400 $\mu$M. $K_m^{(cyt\ c)}$ was found to not vary significantly over the pH range 6.0−9.5, having a value of 2.2 $\mu$M at pH 6.0 and 8.0 and increasing only modestly to 5.5 $\mu$M at pH 9.5 (Table 1). Because of this minimal pH dependence, experiments at additional pHs were deemed unnecessary. In a second set of experiments, the concentration of sulfite was varied while that of cytochrome *c* was held constant at a near-saturating concentration of 15 $\mu$M. In this case, both $k_{cat}$ and $K_m^{sulfite}$ were found to vary significantly over the pH range 6.0−10.0 (Table 1). A plot of $k_{cat}$ versus pH (Figure 3A) is bell-shaped, from which two apparent p$K_a$s, 7.0 ± 0.1 and 10.2 ± 0.2, can be obtained. $k_{cat}/K_m^{sulfite}$ also exhibits a bell-shaped pH dependence (Figure 3B), and again two apparent p$K_a$s can be derived: 6.7 ± 0.1 and 8.4 ± 0.1. Between these two p$K_a$s, a pH optimum of ∼7.8 can be assigned for the enzyme. The results indicate that two apparent ionizations are associated with overall catalysis, one associated with a site that must be deprotonated for the enzyme to be catalytically effective, the other associate with a site that must be protonated. The lower value agrees with that seen in the pH profile for $k_{cat}$, but the higher p$K$ does not, suggesting that different ionization processes are involved in the high- and low-substrate regimes of turnover.

Given the only modest pH dependence of $K_m^{(cyt\ c)}$, values at pH other than 6.0, 8.0, and 9.5 can be interpolated, making it possible to construct a plot of $k_{cat}/K_m^{(cyt\ c)}$ from the present steady-state data. Given the approximately 10-fold smaller values for $K_m^{(cyt\ c)}$ relative to $K_m^{sulfite}$ over the entirety of the pH range 6.0−9.5 investigated here, the magnitude of $k_{cat}/K_m^{(cyt\ c)}$ is comparably about 10-fold greater than that for sulfite $k_{cat}/K_m^{sulfite}$. Again, however, the pH dependence is bell-shaped, with apparent p$K_a$s of 6.7 and 9.4 obtained (Figure 3C). Given the uncertainty introduced by the interpolation involved in determination of $K_m^{(cyt\ c)}$, these p$K_a$s must be regarded as only approximate, although we note that the validity of the interpolation is supported by the observation that $K_d^{(cyt\ c)}$ determined from rapid reaction kinetic studies has a pH dependence comparable to that of $K_m^{(cyt\ c)}$ inferred from the present steady-state data (below).

*Reaction of Oxidized Sulfite Oxidase with Sulfite.* Sulfite oxidase is capable of taking up three reducing equivalents total [two at the molybdenum in going from Mo(VI)) to Mo(IV), and one at the heme], but because sulfite is an obligatory two-electron donor, the reaction of enzyme with an excess of substrate is arrested after the reaction of a single equivalent of sulfite to yield 2-electron reduced enzyme, initially possessing Mo(IV), but after rapid intramolecular electron-transfer possessing Mo(V) and reduced heme to an appreciable degree. The large absorption change associated with reduction of the heme (rate limited by the chemistry at the molybdenum center) provides a convenient experimental handle which can be used to monitor overall enzyme reduction by substrate at the molybdenum center.

Using the absorbance changes at 426 or 410 nm due to reduction of the enzyme heme upon mixing with varying concentrations of sulfite (in pseudo-first-order excess), the effect of pH on the reductive half-reaction of the enzyme was next examined. It is evident from the magnitude of the observed spectral change at all pH values examined that the distribution of reducing equivalents within 2-electron reduced enzyme favors reduced heme and Mo(V) over oxidized heme and Mo(IV) to a significant degree.[3] The anaerobic reduction of enzyme exhibits well-behaved single-exponential kinetics at all substrate concentrations, wavelengths, and pH values between 6.5 and 10.0. At pH 6.0, however, the transients obtained do not fit well to single-, double-, or triple-exponentials, presumably due to protein instability at this low pH; as a result, we limit our analysis to pH 6.5 and above. The dependence of the observed rate constant on

[3] On a much slower time scale than the initial reduction of sulfite oxidase, an intermolecular dismutation reaction is known to take place in which two equivalents of two-electron reduced enzyme are converted to one equivalent each of three- and one-electron reduced enzyme − the latter species is then able to react with a second equivalent of substrate, ultimately yielding a system consisting solely of fully reduced enzyme. This dismutation process is manifested in the present experiments as an extremely slow further reduction of enzyme after the fast phase of the reaction, taking place on a time scale of minutes. From these data (not shown) a second-order rate constant of 360 $M^{-1}s^{-1}$ for the dismutation reaction can be estimated.

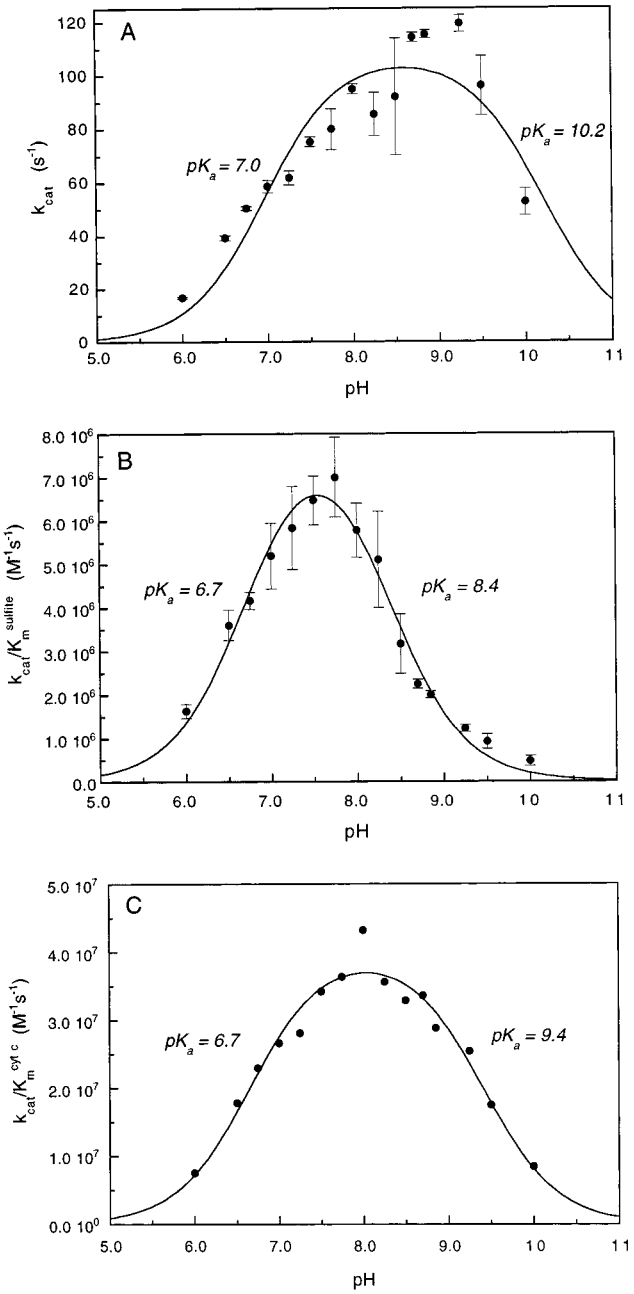


FIGURE 3: The pH dependence of the steady-state kinetic parameters. Panels A−C illustrate the dependence of $k_{cat}$, $k_{cat}/K_M^{sulfite}$ and $k_{cat}/K_m^{(cyt\ c)}$ on pH, respectively. The graph of $k_{cat}$ versus pH (Panel A) fits well to two p$K_a$s, 7.0 and 10.2, and the graph of $K_M$ versus pH fits well to one p$K_a$, 9.0. Experiments were performed in 0.02 M buffer, between pH 6.0 and 10.0, 25 °C, with varying concentrations of sulfite and 15 $\mu$M cytochrome *c*. The dependence $k_{cat}/K_M^{sulfite}$ on pH (panel B) fits well to two p$K_a$s, 6.7 and 8.4. Experiments were performed in 0.02 M buffer, between pH 6.0 and 10.0, 25 °C, with varying concentrations of sulfite and 15 $\mu$M cytochrome *c*.

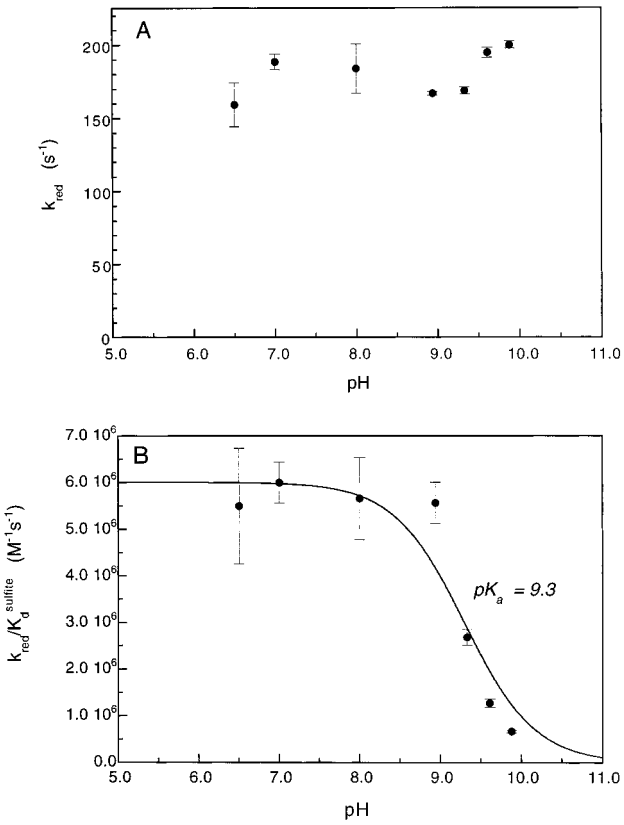


FIGURE 4: The pH dependence of the rapid kinetic parameters for the reductive half reaction. (Panel A) A graph of $k_{red}$ versus pH, indicating the pH independence of this kinetic parameter. Experiments were performed in 0.02 M buffer, between pH 6.5 and 10.0, 25 °C, with varying concentrations of sulfite. The reaction was monitored spectrophotometrically at 426 nm. Panel B, the pH dependence of the effective second-order rate constant $k_{red}/K_d^{sulfite}$. The graph displays the dependence of $k_{red}/K_d^{sulfite}$ on pH and fits well to one p$K_a$, 9.3. Experiments were performed in 0.02 M buffer, between pH 6.5 and 10.0, 25 °C, with varying concentrations of sulfite. The reaction was monitored spectrophotometrically at 426 nm.

sulfite concentration is found to be hyperbolic with a limiting value, $k_{red}$, nearly invariant at 150−200 $s^{-1}$ over the pH range studied (Figure 4A). On the other hand, a plot of $k_{red}/K_d^{sulfite}$ versus pH is sigmoidal, (Figure 4B), yielding a single p$K_a$ of 9.3 ± 0.2, due entirely to the pH dependence of $K_d^{sulfite}$.

Above pH 7.0, $k_{red}$ correlates fairly well in magnitude with $k_{cat}$ (compare the data compiled in Tables1 and 2), although the former parameter is essentially independent of pH. Below pH 7.0, however, $k_{cat}$ becomes significantly smaller than $k_{red}$, indicating that additional processes contribute to the overall kinetic barrier to catalysis. Also, a comparison of $k_{red}/K_d^{sulfite}$ and $k_{cat}/K_m^{sulfite}$ indicates that below pH 7.5 the value of the effective second-order rate constant for the reductive half-reaction is considerably greater than that for steady-state turnover, whereas above pH 7.5 the two parameters are comparable (again, compare the data in Tables 1 and 2). This correlation implies that below pH 7.5 the rate-limiting step for steady-state turnover does not reside in the reductive half-reaction in either the high ($k_{red}$) or low ($k_{red}/K_d^{sulfite}$) substrate concentration regimes. A final observation is that, to the extent that $K_m$ approximates an apparent dissociation constant, both $K_m^{sulfite}$ and $K_d^{sulfite}$ display similar trends (Tables 1 and 2), being essentially constant at approximately 11 $\mu$M below pH 8.0 and increasing above that pH. This serves to justify the above interpolation of values for $K_m^{(cyt\ c)}$ used in the reconstruction of the pH dependence of $k_{cat}/K_m^{(cyt\ c)}$.

*Reaction of Reduced Sulfite Oxidase with Cytochrome c.* By contrast to the reductive half-reaction of sulfite oxidase, the oxidative half-reaction is a necessarily sequential process, as three successive equivalents of cytochrome *c* are required to remove the three reducing equivalents present in fully reduced enzyme. Advantage can be taken of the different spectral changes attributable to cytochrome *c* and the heme

Table 2: Summary of the Rapid Kinetic Parameters for Sulfite Oxidase

| pH | $K_d^{sulfite}$ ($\mu$M) | $k_{red}$ ($s^{-1}$) | $k_{red}/K_d^{sulfite}$ ($M^{-1}$ $s^{-1}$) | $K_d^{(cytochrome\ c)}$ ($\mu$M) | $k_{ox}$ ($s^{-1}$) | $k_{ox}/K_d^{(cytochrome\ c)}$ ($M^{-1}$ $s^{-1}$) |
|---|---|---|---|---|---|---|
| 6.50 | 29 ± 6.0 | 159.5 ± 15 | $5.50 \times 10^6$ | 11.8 ± 4.1 | 129.2 ± 9.9 | $1.09 \times 10^7$ |
| 7.00 | 31.4 ± 2.1 | 188.5 ± 5.3 | $6.00 \times 10^6$ | 17.8 ± 3.1 | 297.7 ± 20.8 | $1.67 \times 10^7$ |
| 8.00 | 32.5 ± 4.1 | 183.9 ± 16.7 | $5.66 \times 10^6$ | 22.1 ± 2.4 | 549.5 ± 25.0 | $2.48 \times 10^7$ |
| 8.94 | 30 ± 2.4 | 167 ± 13.2 | $5.57 \times 10^6$ | 5.2 ± 1.7 | 466.8 ± 30.1 | $8.98 \times 10^7$ |
| 9.33 | 63 ± 3.9 | 169 ± 2.3 | $2.68 \times 10^6$ | 11.6 ± 3.9 | 579.4 ± 59.6 | $4.97 \times 10^7$ |
| 9.61 | 152.9 ± 10.0 | 194.9 ± 3.3 | $1.28 \times 10^6$ | 24.1 ± 5.5 | 578 ± 57.9 | $2.40 \times 10^7$ |
| 9.88 | 299.6 ± 12.2 | 200 ± 2.4 | $6.68 \times 10^5$ | 95.5 ± 26.2 | 473.4 ± 97.5 | $4.96 \times 10^6$ |

center of sulfite oxidase, following the reaction at either 547 (an isosbestic for the enzyme) or 562 nm (an isosbestic for cytochrome *c*), which permits cytochrome reduction and enzyme reoxidation to be followed independently in the course of the reaction. At 547 nm, the anaerobic reduction of cytochrome *c* exhibits well-behaved double-exponential kinetics at all substrate concentrations over the first ~70 ms of the reaction for pHs between 7.0 and 9.0. The same is true at pH 6.0 and 10.0 over the first ~200 ms. At 562 nm, the anaerobic oxidation of enzyme exhibits well-behaved single-exponential kinetics at all substrate concentrations for pHs between 6.0 and 10.0, with rate constants comparable to the faster kinetic phase seen at 547 nm.

At both wavelengths, the observed rate constant (in the case of transients at 547 nm, that of the faster phase) exhibits hyperbolic concentration dependence on the cytochrome *c* concentration. A plot of the observed limiting rate constant for the reaction, $k_{ox}$, versus pH yields a sigmoidal pH dependence (although we note that there is a slight downward trend evident in the data at high pH), with a single apparent p$K_a$ of 6.8 ± 0.4 obtained from a fit to the plot (Figure 5A). This p$K_a$ is very similar to that seen in the steady-state profile for $k_{cat}$ of 7.0. As indicated in Table 2, $K_d^{(cyt\ c)}$ is essentially unchanged between pH 6.0 and 9.0 but begins to increase above this pH. These results are very similar to the trends seen for $K_m^{(cyt\ c)}$ in the steady-state analyses described earlier, serving to justify the assumption made in the steady-state analysis of $k_{cat}/K_m^{(cyt\ c)}$ that the pH dependence of $K_m^{(cyt\ c)}$ is modest over the majority of the pH range investigated here. On the other hand, a plot of $k_{ox}/K_d^{(cyt\ c)}$ versus pH is bell-shaped with two apparent p$K_a$s of 8.0 ± 0.2 and 8.2 ± 0.2 (Figure 5B). The appearance and shape of the $k_{ox}/K_d^{(cyt\ c)}$ plot is generally comparable to that for $k_{cat}/K_m^{(cyt\ c)}$: each fits to two apparent p$K_a$s and shares a common pH optimum of ~8.0 (8.1 for the oxidative half-reaction and 7.8 for the steady-state work). In addition, the effective second-order rate constants for the steady-state turnover and rapid reaction of enzyme with cytochrome *c*, $k_{cat}/K_m^{(cyt\ c)}$ and $k_{ox}/K_d^{(cyt\ c)}$, at pH 6.0, 8.0, and 9.5 possess similar values. These results indicate that the oxidative half-reaction of catalysis contributes significantly to the overall kinetic barrier to catalysis below pH 7.5.

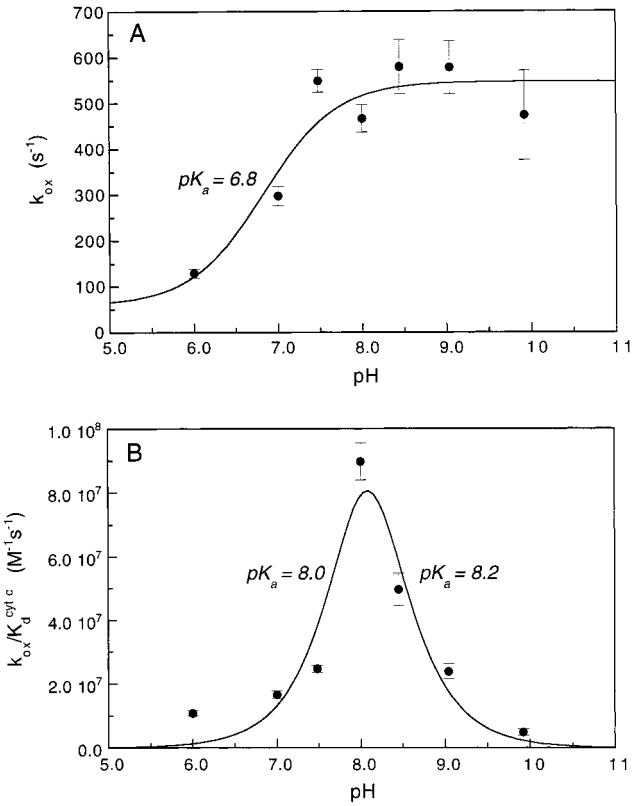


FIGURE 5: The pH dependence of the rapid kinetic parameters for the oxidative half-reaction. (Panel A) The dependence of $k_{ox}$ on pH. The plot fits well to a single p$K_a$ of 6.8. Experiments were performed in 0.02 M buffer, between pH 6.0 and 10.0, 25 °C, with varying concentrations of cytochrome *c*. The reaction was monitored spectrophotometrically at 547 and 562 nm. (Panel B) The pH dependence of the effective second-order rate constant $k_{ox}/K_d^{(cytochrome\ c)}$. The plot fits to two p$K_a$s, 8.0 and 8.2. Experiments were performed in 0.02 M buffer, between pH 6.0 and 10.0, 25 °C, with varying concentrations of cytochrome *c*. The reaction was monitored spectrophotometrically at 547 and 562 nm.

## DISCUSSION

By analogy to mechanisms proposed for the reaction of model Mo(VI)$O_2$ compounds with phosphines (*25*, *26*), we have previously proposed a reaction mechanism for sulfite oxidase in which catalysis is initiated by attack of the sulfite lone pair on one of the Mo═O units of the molybdenum center (*27*, *28*), as shown in Scheme 1. The only indirect role played by the substrate's oxyanion groups in facilitating reaction in the case of sulfite oxidase has been demonstrated, in that methylation of these groups to give dimethylsulfite results in a substantial (300-fold) increase in $K_d$ for the reductive half-reaction at pH 8.0, but only a negligible effect on $k_{red}$ for the reaction. The pH independence of $k_{red}$ seen in the present work is entirely consistent with this chemistry and further indicates that acid−base chemistry is not involved in the breakdown of the $E_{ox}$·sulfite complex.[4] By contrast, the pH dependence of $k_{red}/K_d^{sulfite}$ exhibits a sigmoidal pH profile with an apparent p$K_a$ of 9.3. It is to be emphasized that this kinetic parameter tracks the reaction of free enzyme

[4] We note that the pH independence of $k_{red}$ is not inconsistent with other mechanisms that have been proposed for sulfite oxidase, particularly those involving direct coordination of sulfite to the active site molybdenum, and our present results in themselves to not discriminate between these. In light of our work with dimethylsulfite cited above, however, these mechanisms are deemed unlikely.

Scheme 1: Proposed Reaction Mechanism for the Reductive Half-Reaction of Sulfite Oxidase

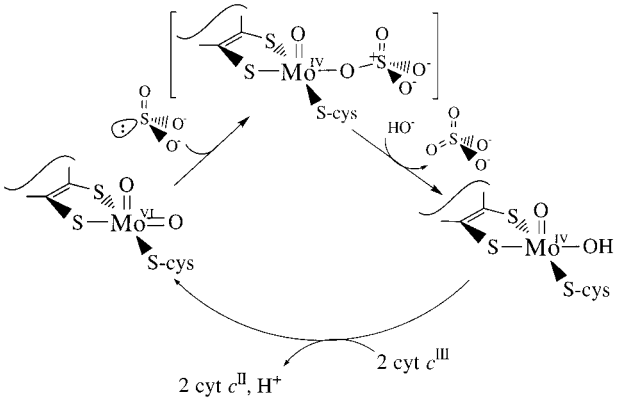


with free substrate in the low-substrate concentration regime through to the first irreversibly formed intermediate in the reductive half-reaction, and its pH profile reflects ionizations in the free enzyme and free substrate. The observed p$K_a$ of 9.3 is consistent with that for a tyrosine residue and may reflect the ionization of Tyr 322, which has been shown from the X-ray crystal structure of the enzyme to constitute part of the substrate binding site of sulfite oxidase (*29*, *30*). Deprotonation of this residue would reasonably be expected to compromise binding of the negatively charged substrate. It is interesting to note that the ionization of substrate from the mono- to dianion (p$K_a$ = 6.91; ref *31*) is not evident in the pH profile of $k_{red}/K_d^{sulfite}$, indicating that the enzyme does not discriminate between these two ionization states of free substrate (at least not in a way that influences this kinetic parameter). This interpretation in turn implies that the apparent p$K_a$ associated with the acidic limb of the pH profile for the steady-state kinetic parameter $k_{cat}/K_m^{sulfite}$ does not reside in the reductive half-reaction of the catalytic cycle. Given the manner in which we are following the kinetics of the reductive half-reaction, by means of the spectral change associated with heme reduction, it is to be emphasized that any pH dependence intrinsic to electron transfer from the molybdenum to the heme must also be manifested in the pH profile for $k_{cat}/K_m^{sulfite}$. The implication is that the apparent p$K_a$ of 6.7 in the pH profile for $k_{red}/K_d^{sulfite}$ must arise from the oxidative half-reaction of the catalytic sequence (see below).

The pH profile for $k_{ox}$, reflecting the limiting rate constant associated with electron transfer from the heme group of sulfite oxidase to cytochrome *c* within the protein:protein complex, exhibits an apparent p$K_a$ of 6.8. Inspection of the profile indicates that the low pH limit for $k_{ox}$ is approximately 60 $s^{-1}$, implying that deprotonation of the group responsible for this p$K_a$ facilitates electron transfer to cytochrome *c*, but is not strictly required for it. In the absence of a concrete structural model for the protein:protein complex, it is not possible to put forward a specific electron-transfer pathway and identify which ionizable group along this path might be responsible for this ionization.

The pH profile for $k_{ox}/K_d^{(cyt\ c)}$, reflecting the second-order rate constant for intermolecular electron transfer from sulfite oxidase to cytochrome *c* in the low [cytochrome *c*] limit, exhibits a bell-shaped profile with two essentially equal apparent p$K_a$s of 8.0 and 8.2.[5] Given the close spacing of these two values, it is not possible to say with confidence whether each arises from discrete ionizations of individual sites or represents composites of multiple sites. There are several ionizable residues on the surface of the heme domain of sulfite oxidase which (by virtue of proximity to the exposed heme edge) presumably interacts with cytochrome *c*, including His 69, Tyr 62, Lys 46, Glu 67, and Asp 45, as well as the heme propionate groups. Given the existing evidence indicating that a cluster of lysine residues around the exposed heme edge of cytochrome *c* is responsible for electrostatic interactions between the electron carrier and its physiological partners and that Lys 13, 27, 72, and 86 are specifically involved in the interaction with sulfite oxidase (*4*), it is most likely that the residues on sulfite oxidase are negatively charged and therefore deprotonated for favorable interaction with cytochrome *c*. Accordingly, this suggests that His 69 and/or Tyr 62 are responsible for the acid limb of the curve, but obviously it remains for future work to establish whether this is the case. The residues responsible for the basic limb of the profile, which must be protonated for effective intermolecular transfer between the two proteins, are more difficult to identify, but possibly represent either lysine residues on cytochrome *c* or a group on sulfite oxidase involved with an interaction with a negatively charge (or hydrogen-bonding acceptor) on cytochrome *c*. A p$K_a$ of 8.2 is quite low for a lysine residue but is not completely unreasonable and may possibly be the result of so many lysine residues being in close proximity to the heme edge of cytochrome *c*.

With the above, it is possible to rationalize the steady-state kinetic behavior of sulfite oxidase, at least qualitatively, in the context of the reductive and oxidative half-reaction kinetics. Considering first $k_{cat}$ for the high substrate concentration regime, it is evident that over the pH range 7−9 this steady-state parameter is significantly smaller than $k_{ox}$, but within a factor of 2 of $k_{red}$. Below pH 7, $k_{cat}$ becomes significantly smaller than $k_{red}$; while the form of the profile in this pH region resembles that for $k_{ox}$, the magnitude of $k_{ox}$ remains at least a factor of 5 greater than that for $k_{cat}$. In making quantitative comparisons between the steady-state and rapid reaction kinetic parameters, it is important to recognize that the intrinsic rates of reaction for oxidized enzyme with sulfite and the first equivalent of cytochrome *c* with fully reduced cytochrome *c* are not likely to pertain directly to protein in the steady state, as enzyme in the steady-state is neither fully oxidized nor fully reduced. As has been shown for systems related to sulfite oxidase (*17*), to the extent that the partially reduced enzyme accumulating in the steady state possesses a reduced molybdenum center or an oxidized heme, it will not be able to participate in both half-reactions of the catalytic sequence and thus will be catalytically inert. The result is that, in reconciling the steady state and rapid reaction kinetics, the intrinsic rate constant determined for each half-reaction must be attenuated to account for that portion of enzyme in the steady-state population possessing an unfavorable electron distribution for catalysis. In some cases, the effect can be an order or magnitude or more. This

[5] In earlier work, Eltis et al. (*32*) calculated a second-order rate constant for the oxidation of bovine ferricytochrome $b_5$ with a pseudo first-order excess of cytochrome *c* to be $2.0 \pm 0.2 \times 10^7$ $M^{-1}$ $s^{-1}$ at pH 7.0. This value is comparable to the $1.67 \times 10^7$ $M^{-1}$ $s^{-1}$ calculated for $k_{ox}/K_d^{cyt\ c}$ for sulfite oxidase at pH 7.0, indicating that sulfite oxidase is almost as efficient at reducing cytochrome *c* as the smaller protein system.

being the case, we consider it likely that the pH profile for $k_{cat}$ in the pH region 6−8 is due to the pH dependence of $k_{ox}$ over this range, attenuated by a factor of approximately 5 for the above reasons.

For the low substrate concentration regimes, it is necessary to compare $k_{cat}/K_m^{sulfite}$ with $k_{red}/K_d^{sulfite}$, on one hand, and $k_{cat}/K_m^{(cyt\ c)}$ with $k_{red}/K_d^{(cyt\ c)}$ on the other.[6] It is evident that the maximum values for $k_{cat}/K_m^{sulfite}$ with $k_{red}/K_d^{sulfite}$ are in good agreement, at approximately $6 \times 10^7$ $M^{-1}$ $s^{-1}$. On the other hand, $k_{cat}/K_m^{sulfite}$ decreases sharply below pH 7.0 (with the profile governed by two p$K_a$s of 6.7 and 8.4) while $k_{red}/K_d^{sulfite}$ remains essentially constant at its maximum value over this pH range (governed by a single p$K_a$ of 9.3).[7] This indicates that the low-pH limb of the $k_{cat}/K_m^{sulfite}$ plot arises from ionizations in the oxidative rather than reductive half-reaction. Indeed, $k_{ox}/K_d^{(cyt\ c)}$ is bell-shaped, as is $k_{cat}/K_m^{(cyt\ c)}$; as in the case of the reductive half-reaction, the maximum values for these two parameters are similar but a factor of 5−10 above the comparable values for the reductive half-reaction over most of the pH range (owing the smaller $K_d$ for cyt *c* relative to sulfite). It is only below pH 7, where the pH dependence of $k_{cat}/K_m^{sulfite}$ and $k_{red}/K_d^{sulfite}$ diverge in the reductive half-reaction, that $k_{ox}/K_d^{(cyt\ c)}$ becomes comparable in value to $k_{red}/K_d^{sulfite}$. This again implies that except at low pH the reductive half-reaction constitutes the principal kinetic barrier to catalysis. We note that close inspection of the two bell-shaped curves indicates that the pH profiles for the two oxidative half-reaction parameters $k_{ox}/K_d^{(cyt\ c)}$ and $k_{cat}/K_m^{(cyt\ c)}$ are in fact quite distinct, with apparent p$K_a$s of 8.0 and 8.2 associated with $k_{ox}/K_d^{(cyt\ c)}$ from the rapid reaction experiments and values of 6.7 and 9.4 for $k_{cat}/K_m^{(cyt\ c)}$ from the steady-state data. The maximum value for the steady-state parameter is also approximately half that for the rapid reaction parameter. These apparent disparities ultimately have to do with the fact that the steady-state term must contain contributions from the reductive as well as the oxidative half-reaction, with the former contributing to the overall kinetic barrier to turnover in the steady-state reaction.

Electron transfer in one-electron reduced sulfite oxidase has been found to be very rapid at most pH values (1600 $s^{-1}$ at pH 6.0, 2400 $s^{-1}$ at pH 7.0, but decreasing to 60 $s^{-1}$ at pH 9.0; refs *14* and *15*). It must be recognized, however, that this rate involves the Mo(VI/V) couple in one-electron reduced enzyme, rather than the Mo(V/IV) couple as must be the case within the two-electron reduced enzyme, and the catalytic relevance of so low a rate constant must be regarded with caution. Indeed, the present experiments also show that $k_{red}$, which has a requisite electron-transfer event before an absorbance change can be detected, and $k_{cat}$ are greater than the 60 $s^{-1}$ at pH 9.0. (By contrast, the $k_{ox}$ determined from the fast phase of the reaction in these experiments represents the conversion of fully reduced enzyme to two-electron reduced enzyme, so intramolecular electron transfer is not integral to this kinetic parameter.)

Using beef liver sulfite oxidase, Speck et al. (*4*) reported a steady-state analysis of the enzyme over the pH range 6.0−8.5, varying cytochrome *c* at a fixed sulfite concentration of 2.5 mM. In reporting their data as a set of nested Eadie-Hofstee plots, however, it is difficult to ascertain the pH dependence of $k_{cat}$ and $k_{cat}/K_m^{(cyt\ c)}$, and in any case the work was performed in buffer that contained 50 mM chloride, well above the $K_i$ for this anion of 4 mM. The work presented here represents a detailed kinetic analysis of sulfite oxidase over the pH range 6.5−10, involving both steady-state and rapid kinetic studies, under conditions where the anion composition of the various buffers is tightly controlled (Rajagopalan, 1980). From a comparison of the pH profiles of the effective second-order rate constant terms $k_{cat}/K_m^{sulfite}$ and $k_{cat}/K_m^{(cyt\ c)}$, it is evident that above pH 7.5, catalysis is principally rate limited by the reductive half-reaction, but below pH 7.5, the oxidative half-reaction contributes to the overall kinetic barrier to catalysis. At high pH, intramolecular electron transfer between the molybdenum and heme centers may also contribute to this barrier. Our results (1) support the general reaction mechanism we have previously proposed; (2) suggest a key role for ionization of Tyr 322, found in the substrate-binding pocket of sulfite oxidase, in catalysis; (3) indicate that the enzyme does not discriminate between the mono- and dianionic forms of substrate; and (4) indicate that the reductive half-reaction is principally rate limiting, but that below pH 7.5 the oxidative half-reaction contributes significantly and accounts for the overall pH dependence of turnover.

[6] In these experiments, the enzyme may be assumed to be largely oxidized in the steady-state under conditions of saturating [cytochrome *c*] and low [sulfite], and largely reduced at saturating [sulfite] and low [cytochrome *c*]. In the limit of these two cases, the above kinetic attenuation effects must asymptote to zero.

[7] In EPR studies by Cohen et al. (*3*) and Bray et al. (*23*), the $Mo^V$ signal is found to vary significantly with pH. The $Mo^V$ form of sulfite oxidase is known to adopt different structures at low and high pH's, with the different EPR signals designated "low pH" and "high pH", respectively. Cohen et al. (*3*) determined that these species interconvert with an apparent p$K_a$ of 8.2 in 0.1 M Tris/HCl buffers. Bray et al. (*23*) extended this study another step and found that the p$K_a$ shifts from 7.0 to 8.1 to 9.0 as the anionic concentration of chloride is raised from 0 mM to 10 mM to 100 mM. It is difficult to relate these p$K_a$s (relating to the Mo(V) oxidation state) to the kinetically determined values reported here for the reductive half-reaction (necessarily relating to the Mo(VI) oxidation state), given the well-known thermodynamic linkage of oxidation state changes with degree of protonation for a variety of molybdenum systems (*33, 34*).

## REFERENCES


1. Hille, R. (1996) *Chem. Rev. 96*, 2757−2816.
2. Howell, L. G., and Fridovich, I. (1968) *J. Biol. Chem. 243*, 5941−5947.
3. Cohen, H. J., Betcher-Lange, S., Kessler, D. L., and Rajagopalan, K. V. (1972) *J. Biol. Chem. 247*, 7759−7766.
4. Speck, S. H., Koppenol, W. H., Dethmers, J. K., Osheroff, N., Margoliash, E., and Rajagopalan, K. V. (1981) *J. Biol. Chem. 256*, 7394−7400.
5. Kessler, D. L., and Rajagopalan, K. V. (1972) *J. Biol. Chem. 247*, 6566−6573.
6. Kessler, D. L., and Rajagopalan, K. V. (1974) *Biochim. Biophys. Acta 370*, 389−398.
7. Rajagopalan, K. V. (1980) in *Molybdenum and Molybdenum Containing Enzymes* (Coughlan, M., Ed.) pp 243−272, Pergamon Press, New York.
8. Ratnam, K., Brody, M. S., and Hille, R. (1996) *Prepr. Biochem. Biotech. 26*, 143−154.
9. Zehnder, A. J. B., and Wuhrmann, K. (1976) *Science 194*, 1165−1166.
10. Lehman, T. C., Hale, D. E., Bhala, A., and Thorpe, C. (1990) *Anal. Biochem. 186*, 280−284.
11. Lehman, T. C., and Thorpe, C. (1990) *Biochemistry 29*, 10594−10602.
12. Massey, V. (1959) *Biochim. Biophys. Acta 34*, 255−256.

13. Bradford, M. M. (1976) *Anal. Biochem. 72*, 248−254.
14. Sullivan, E. P., Jr., Hazzard, J. T., Tollin, G., and Enemark, J. H. (1992) *J. Am. Chem. Soc. 114*, 9662−9663.
15. Sullivan, E. P., Jr., Hazzard, J. T., Tollin, G., and Enemark, J. H. (1993) *Biochemistry 32*, 12465−12470.
16. Bevington, P. R. (1969) *Data Reduction and Error Analysis for the Physical Sciences*, McGraw-Hill, Inc., New York.
17. Hille, R., and Massey, V. (1991) *J. Biol. Chem. 266*, 17401−17408.
18. Huang, L., Rohlfs, R. J., and Hille, R. (1995) *J. Biol. Chem. 270*, 23958−23965.
19. Strickland, S., Palmer, G., and Massey, V. (1975) *J. Biol. Chem. 250*, 4048−4052.
20. Cohen, H. J., and Fridovich, I. (1971) *J. Biol. Chem. 246*, 359−366.
21. Garrett, R. M., and Rajagopalan, K. V. (1996) *J. Biol. Chem. 271*, 7387−7391.
22. Gutteridge, S., Lamy, M. T., and Bray, R. C. (1980) *Biochem. J. 191*, 285−288.
23. Bray, R. C., Gutteridge, S. J., Lamy, M. T., and Wilkinson, T. (1983) *Biochem. J. 211*, 227−236.
24. George, G. N., Prince, R. C., Kipke, C. A., Sunde, R. A., and Enemark, J. H. (1988) *Biochem. J. 256*, 307−309.
25. Caradonna, J. P., Reddy, P. R., and Holm, R. H. (1988) *J. Am. Chem. Soc. 110*, 2139.
26. Pietsch, T., and Hall, M. (1996) *Inorg. Chem. 35*, 1273.
27. Hille, R. (1994) *Biochim. Biophys. Acta 1184*, 143−169.
28. Brody, M. S., and Hille, R. (1995) *Biochim. Biophys. Acta 1253*, 133−135.
29. Kisker, C., Schindelin, H., Pacheco, A., Wehbi, W. A., Garrett, R. M., Rajagopalan, K. V., Enemark, J. H., and Rees, D. C. (1997) *Cell 91*, 973−983.
30. Kisker, C., Schindelin, H., and Rees, D. C. (1997) *Annu. Rev. Biochem. 66*, 233−267.
31. Weast, R. C. (1971) CRC Handbook, 51st ed. (Weast), p D121, Chemical Rubber Co., Cleveland.
32. Eltis, L. D., Herbert, R. G., Barker, P. D., Mauk, A. G., and Northrup, S. H. (1991) *Biochemistry 30*, 3663−3674.
33. Stiefel, E. I. (1973) *Proc. Natl. Acad. Sci. U.S.A. 70*, 988.
34. Stiefel, E. I. (1977) *Prog. Inorg. Chem. 21*, 1.

BI9902539